

# POSSIBILITIES AND LIMITS OF EXPERIMENTAL RESULTS IN THE INVESTIGATION OF REACTION DYNAMICS IN HEAVY ION REACTIONS\*

A. ANASTASI<sup>a,b</sup>, F. CURCIARELLO<sup>a,c,d</sup>, G. FAZIO<sup>a</sup>, G. GIARDINA<sup>a</sup>  
G. MANDAGLIO<sup>a,c</sup>, A.K. NASIROV<sup>e,f</sup>

<sup>a</sup>Dipart. di Fisica e di Scienze della Terra, University of Messina, Messina, Italy

<sup>b</sup>INFN Laboratori Nazionali di Frascati, Frascati, Italy

<sup>c</sup>INFN Gruppo Collegato di Messina, Messina, Italy

<sup>d</sup>Novosibirsk State University, 630090 Novosibirsk, Russia

<sup>e</sup>JINR — Bogoliubov Laboratory of Theoretical Physics, Dubna, Russia

<sup>f</sup>Institute of Nuclear Physics, Tashkent, Uzbekistan

(Received November 17, 2015)

The theoretical results of the individual  $xn$ ,  $\alpha xn$ ,  $pxn$ ,  $p\alpha xn$ , and  $2\alpha xn$  evaporation residue excitation functions in the  $^{16}\text{O}+^{204}\text{Pb}$ ,  $^{40}\text{Ar}+^{180}\text{Hf}$ ,  $^{82}\text{Se}+^{138}\text{Ba}$ , and  $^{124}\text{Sn}+^{92}\text{Zr}$  reactions leading to the  $^{220}\text{Th}$  compound nucleus are presented and analyzed with the aim to study the entrance channel effects on the evaporation residue yields. The comparison of the complete theoretical results with the available experimental determinations shows a large difference connected with the unknown and unidentified nuclei of the total ER production. Such a difference between experimental and theoretical results also appears clearly by comparing the trend of the  $\sigma_{\text{ER}xn}/\sigma_{\text{ERtot}}$  ratio as a function of the excitation energy of the compound nucleus for the investigated reactions.

DOI:10.5506/APhysPolBSupp.8.583

PACS numbers: 25.70.Jj, 25.70.Gh

## 1. Introduction

We study  $^{16}\text{O}+^{204}\text{Pb}$ ,  $^{40}\text{Ar}+^{180}\text{Hf}$ ,  $^{82}\text{Se}+^{138}\text{Ba}$ , and  $^{124}\text{Sn}+^{92}\text{Zr}$  reactions leading to the  $^{220}\text{Th}$  compound nucleus (CN) because such a set of four reactions ranges from a very mass asymmetric reaction to an almost mass symmetric one. Therefore, it is possible to investigate the dynamic effects of the entrance channel on the evaporation residue nuclei (ERs) formation for which already exist in literature [1–4] experimental results of ERs

---

\* Presented at the XXII Nuclear Physics Workshop “Marie and Pierre Curie”, Kazimierz Dolny, Poland, September 22–27, 2015.

yields of the above-mentioned reactions. For these nuclear reactions leading to the same  $^{220}\text{Th}^*$  CN, we presented in Ref. [5] a study regarding the entrance channel effects of reactions with different mass asymmetries on the capture of projectile by the target nucleus, complete fusion in competition with quasifission process at the first stage of reaction, and the competition between fission and evaporation residue (ER) processes at the last stage of reaction during the de-excitation cascade of CN. The method of calculation and the reliable theoretical results have been presented and discussed in [5] and references therein [6–11]. Instead, in the present paper, we would like to discuss the limits about the use of experimental results of evaporation residue excitation functions obtained for various nuclear reactions with different entrance channels, with the aim of obtaining information about the dynamical effects of entrance channels on the ERs yields by observing the  $\sigma_{\text{ER}xn}/\sigma_{\text{ERtot}}$  ratios *vs.*  $E_{\text{CN}}^*$  for the various reactions leading to the same CN formation.  $\sigma_{\text{ER}xn}$  represents the cross sections of all ER nuclei reached after neutron emission only from the de-excitation cascade of CN, and  $\sigma_{\text{ERtot}}$  represents the total cross section of ERs nuclei when all contributions of charged particle emission are also included along the de-excitation cascade of CN;  $E_{\text{CN}}^*$  represents the excitation energy of the  $^{220}\text{Th}^*$  CN formed in each considered reaction.

In Sect. 2, we present and discuss the experimental results presented in literature [1–4] and the comparison with the results obtained by us for the  $^{16}\text{O}+^{204}\text{Pb}$ ,  $^{40}\text{Ar}+^{180}\text{Hf}$ ,  $^{82}\text{Se}+^{138}\text{Ba}$ , and  $^{124}\text{Sn}+^{92}\text{Zr}$  investigated reactions. In Sect. 3, we give our conclusions.

## 2. Comparison between experimental and theoretical results

The main motivation of the present paper is the investigation of the limits of experimental results of identifying all the ER nuclei produced in various reactions, in order to study their dependence on the entrance channel. We draw attention to Fig. 1 (a) presenting the contents of Fig. 3 of the paper published by Hinde *et al.* [4].

The authors affirmed that no consistent trend for  $\sigma_{xn}/\sigma_{\text{ER}}$  ratios appear as a function of mass asymmetry for reactions induced by heavier beams, while for the reactions induced by  $^{16}\text{O}$  the  $\sigma_{xn}/\sigma_{\text{ER}}$  ratio is substantially lower than for the other reactions, because for the  $^{16}\text{O}+^{204}\text{Pb}$  reaction the eventual contribution of the incomplete fusion process with  $\alpha$ -particle as spectator leads to an increase of the  $\alpha$  yields, determining a suppression of the  $\sigma_{xn}/\sigma_{\text{ER}}$  ratio.

We were intrigued by these experimental results together with the conclusion, also because the same experimental results reported by us in Fig. 1 (b) gave indications of the appreciable different trends in the  $\sigma_{\text{ER}xn}/\sigma_{\text{ERtot}}$  ra-

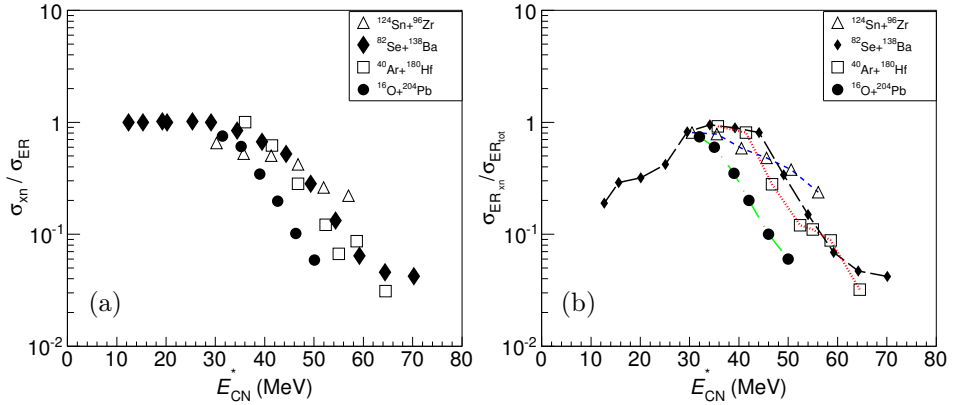


Fig. 1. (a) The  $\sigma_{xn}/\sigma_{ER}$  ratio vs. the  $E^*$  excitation energy of the  $^{220}\text{Th}^*$  CN, for the  $^{124}\text{Sn}+^{92}\text{Zr}$ ,  $^{82}\text{Se}+^{138}\text{Ba}$ ,  $^{40}\text{Ar}+^{180}\text{Hf}$  and  $^{16}\text{O}+^{204}\text{Pb}$  reactions, as presented in [4]; (b) as in (a) but presented by us by using directly the experimental data reported in: [1] open triangles, [2] full diamonds, [3] open squares, [4] full circles. In panel (b), the labels  $\sigma_{ER,xn}$  and  $\sigma_{ER,tot}$  correspond to the labels  $\sigma_{xn}$  and  $\sigma_{ER}$  used in panel (a), respectively; each line connecting experimental points is a guide for the eye.

tio values vs.  $E_{CN}^*$  for the four considered reactions. Moreover, it is needed to take into account that the experimental method has a real time limit of about some  $\mu\text{s}$  for the identification of the ER nuclei. Due to this restriction in the registration of the short living reaction products, many unknown contributions are missing in the collected data. Therefore, we were encouraged to study the above-mentioned nuclear reactions and to analyze our theoretical results.

By analyzing the formation of the dinuclear system (DNS) at first stage of the projectile–target collision and its evolution to the CN in competition with the quasifission and fast fission processes, we obtain the excitation functions of the ER nuclei formed along the de-excitation cascade of the heated CN by evaporation of neutral and charged particles in competition with the fission process.

The details of our method and the results of cross sections obtained for the four considered reactions with different mass asymmetry in the entrance channel leading to the same  $^{220}\text{Th}^*$  CN are described in [5]. Therefore, in the following, we present in Figs. 2, 3, 4, and 5 the calculated individual  $xn$ ,  $\alpha xn$ ,  $pxn$ ,  $pa xn$ , and  $2\alpha xn$  ER excitation functions (see panels (a) of the figures) together with the  $\sigma_{ER,xn}/\sigma_{ER,tot}$  ratios vs.  $E_{CN}^*$  (see panels (b) of the figures) for the  $^{16}\text{O}+^{204}\text{Pb}$ ,  $^{40}\text{Ar}+^{180}\text{Hf}$ ,  $^{82}\text{Se}+^{138}\text{Ba}$ , and  $^{124}\text{Sn}+^{92}\text{Zr}$  reactions, respectively.

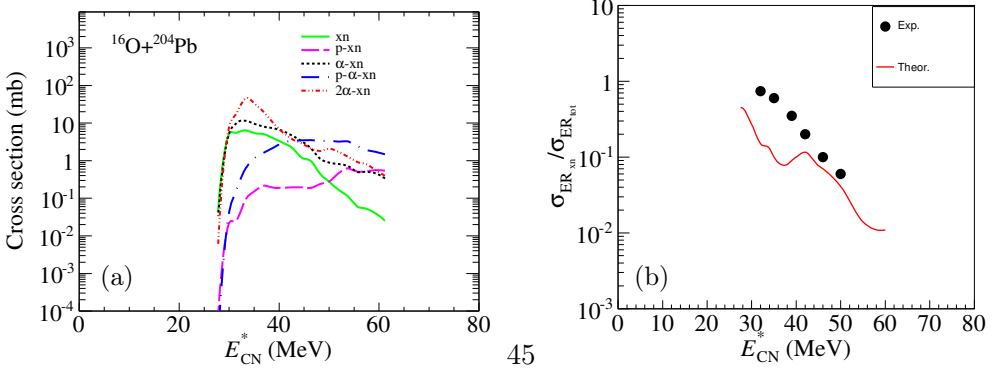


Fig. 2. (a) Theoretical ER excitation functions of the individual  $xn$  (solid line),  $p xn$  (dashed),  $\alpha xn$  (dotted),  $p\alpha xn$  (dash-dotted), and  $2\alpha xn$  (dash-double dotted) contributions for the  $^{16}\text{O} + ^{204}\text{Pb}$  reaction in the  $E_{\text{lab}} = 78\text{--}115$  MeV beam energy range. (b) The  $\sigma_{\text{ER}xn}/\sigma_{\text{ERtot}}$  ratio values vs.  $E_{\text{CN}}^*$  for this reaction: full line represents the theoretical trend, full points represent the experimental determinations [4].

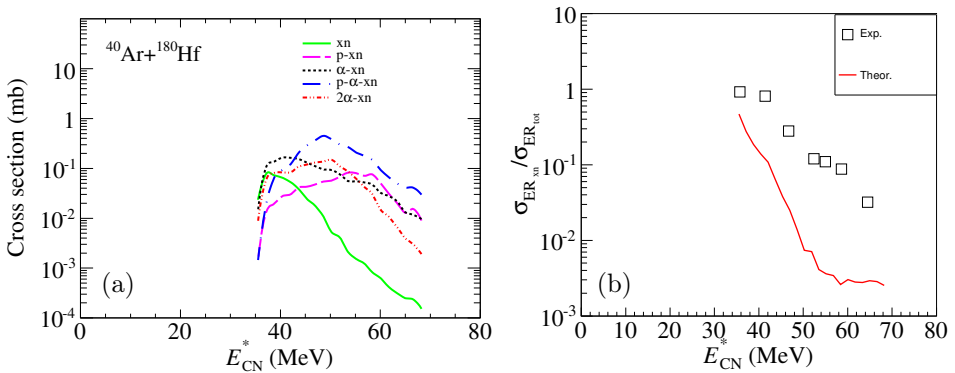


Fig. 3. As in Fig. 2 but for the  $^{40}\text{Ar} + ^{180}\text{Hf}$  reaction in the  $E_{\text{lab}} = 165\text{--}212$  MeV beam energy range. The total experimental ER determinations are taken from Ref. [3].

As these figures show, there are some similar trends for the ER excitation functions found for the considered reactions, for example, the shape of the  $xn$  contribution, the modest  $p xn$  contribution up to about  $E_{\text{CN}}^* = 45$  MeV, the important  $\alpha xn$  contribution up to about  $E_{\text{CN}}^* = 65$  MeV, while there are important differences among the shapes and details for the other ER excitation functions. For example, the  $2\alpha xn$  contribution is large for the  $^{16}\text{O} + ^{204}\text{Pb}$  reaction, while it remains important also for the other reactions but with some specific details. The  $p\alpha xn$  contribution is important at higher

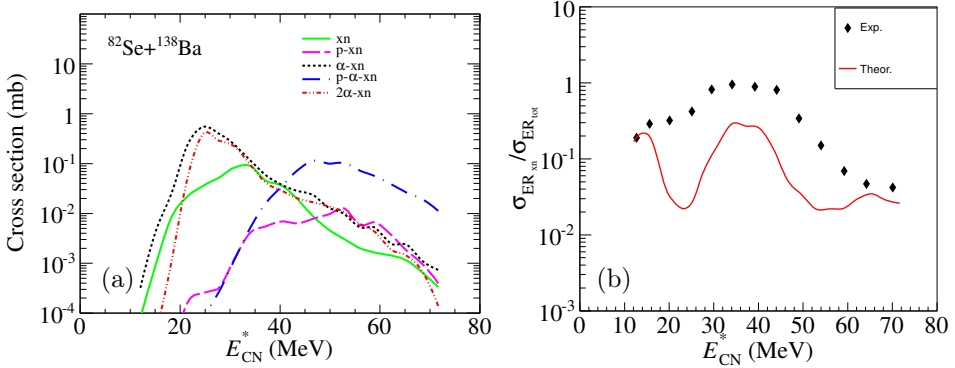


Fig. 4. As in Fig. 2 but for the  $^{82}\text{Se} + ^{138}\text{Ba}$  reaction in the  $E_{\text{lab}} = 307\text{--}402$  MeV beam energy range. The total experimental ER determinations are taken from Ref. [2].

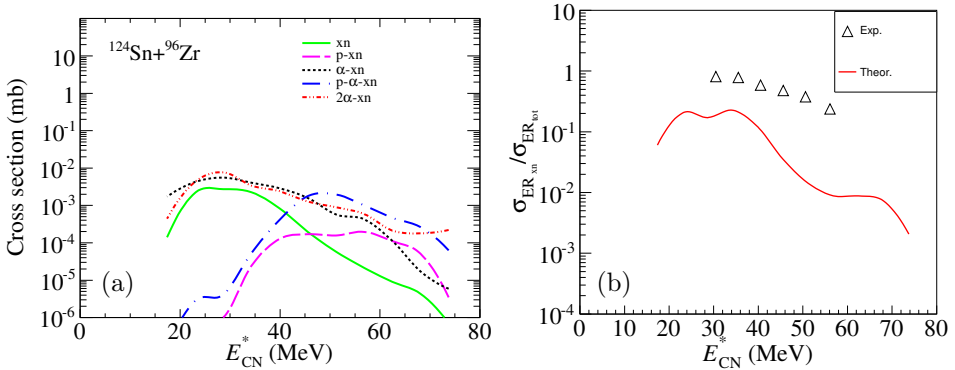


Fig. 5. As in Fig. 2 but for the  $^{124}\text{Sn} + ^{96}\text{Zr}$  reaction in the  $E_{\text{lab}} = 471\text{--}600$  MeV beam energy range. The total experimental ER determinations are taken from Ref. [1].

$E_{\text{CN}}^*$  energies and certainly it is dominant at energies higher than 45 MeV for all considered reactions. In fact, if we observe the calculated ER excitation functions *vs.*  $E_{\text{CN}}^*$  for the four considered reactions (see panel (a) of Figs. 2, 3, 4, and 5), we can clearly note the considerable specific effects of the entrance channel on the ER nuclei formation: the calculated  $\sigma_{\text{ER,tot}}$  excitation functions for the investigated reactions are higher than the ones obtained in experiments by the all possible identified ER nuclei. Moreover, if we look at the panel (b) of the same figures, we observe for the four reactions the important differences between the effective theoretical  $\sigma_{\text{ER,xn}}/\sigma_{\text{ER,tot}}$  ratios *vs.*  $E_{\text{CN}}^*$  (full line) and the corresponding ratio values obtained in experiments (full points). We show this important result in Figs. 6 and 7 related

to a mass asymmetric reaction (for example  $^{40}\text{Ar}+^{180}\text{Hf}$ ) and an almost mass symmetric reaction (for example  $^{82}\text{Se}+^{138}\text{Ba}$ ), where the yields of the theoretical  $\sigma_{\text{ERtot}}$  calculated by us are considerably higher than the ones of the experimental  $\sigma_{\text{ERtot}}$  values determined through the all possible identified ER nuclei. The ratio between the yields ranges within factors of 2–10 times in the complete explored  $E_{\text{CN}}^*$  excitation energy interval for the reaction induced by  $^{40}\text{Ar}$ , and factors of 2–20 times in the 17–55 MeV energy interval for the reaction induced by  $^{82}\text{Se}$ .

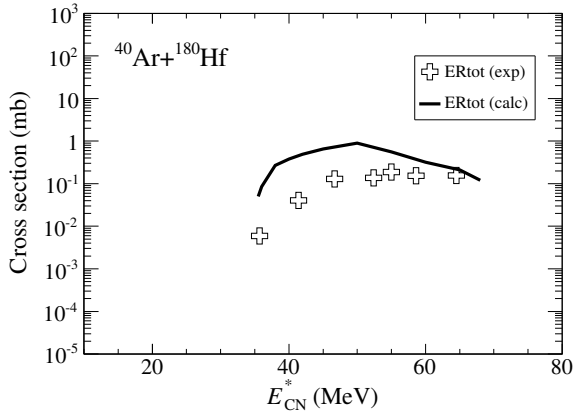


Fig. 6. The full line represents the sum ( $\sigma_{\text{ERtot}}$ ) of the total calculated individual ER contributions for the  $^{40}\text{Ar} + ^{180}\text{Hf}$  reaction; the open cross symbols represent the total experimental ER determinations Ref. [3].

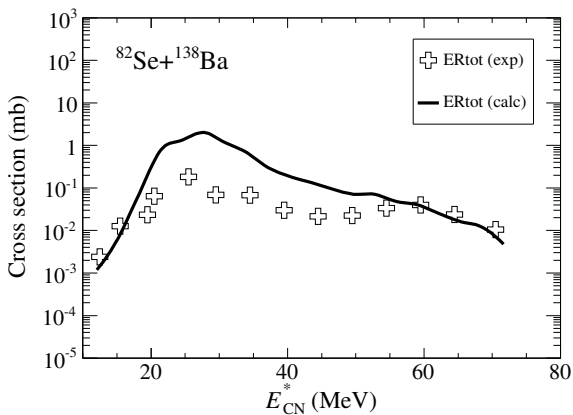


Fig. 7. As in Fig. 6 but for the  $^{82}\text{Se} + ^{138}\text{Ba}$  reaction. The total experimental ER determinations are taken from Ref. [2].

### 3. Conclusions

Our analysis of the four considered investigated reactions forming the  $^{220}\text{Th}^*$  CN allows us to reach a reliable understanding of the entrance channel effects on the compound nucleus formation and consequently on the evaporation residue nuclei production. Such effects are revealed in the stage of the DNS formation at the capture, in the competition of the quasifission and fusion processes at first stage of reaction, and then to the competition of the fission and evaporation processes at de-excitation cascade of CN in the last stage of reaction. The determination by experiments of the cross section of the possible identified residue nuclei after evaporation from CN of neutral and charged particles is useful but the measured data can be not enough to establish the true rate of the complete ER production. Therefore, each kind of the individual ER excitation function is characterized by the reaction entrance channels and by the excitation energy range of the reached compound nucleus with the same charge  $Z$  and mass  $A$  values. At the same time, the other important dynamical properties can be different, even if the CN is formed with the same  $E_{\text{CN}}^*$  excitation energy. Therefore, a detailed analysis of the reaction dynamics due to the collision of nuclei in the entrance channel is possible only through the use of an appropriate, and refined theoretical model suitable to provide sensitive and reliable results characterizing the corresponding reaction mechanism.

### REFERENCES

- [1] C.C. Sahm *et al.*, *Nucl. Phys. A* **441**, 316 (1985).
- [2] K. Satou *et al.*, *Phys. Rev. C* **65**, 054602 (2002).
- [3] D. Vermeulen *et al.*, *Z. Phys. A* **318**, 157 (1984).
- [4] D.J. Hinde *et al.*, *Phys. Rev. Lett.* **89**, 282701 (2002).
- [5] K. Kim *et al.*, *Phys. Rev. C* **91**, 064608 (2015).
- [6] G. Fazio *et al.*, *Mod. Phys. Lett. A* **20**, 391 (2005).
- [7] G. Fazio *et al.*, *J. Phys. Soc. Jpn.* **77**, 124201 (2008).
- [8] G. Mandaglio *et al.*, *Phys. At. Nucl.* **72**, 1639 (2009).
- [9] A.K. Nasirov *et al.*, *Phys. Rev. C* **79**, 024606 (2009).
- [10] A.K. Nasirov *et al.*, *Phys. Lett. B* **686**, 72 (2010).
- [11] G. Mandaglio *et al.*, *Phys. Rev. C* **86**, 064607 (2012).